

Microstructure and Young's Modulus of $(\text{TiZr})_{2-x}(\text{NbTaMo})_x$ Bio-High Entropy Alloys

Mitsuharu Todai^{1,a*}, Nagi Takahashi^{1,b}, Neiro Tanaka^{1,c}, Daisuke Tanaka^{2,d}, Takeshi Nagase^{3,e}, Aira Matsugaki^{4,f}, Takayoshi Nakano^{4,g}

¹Department of Environmental Materials Engineering, National Institute of Technology, Niihama College, 7-1 Yagumo-cho Niihama, Ehime 792-8580, Japan

²Graduate School of Information Sciences, Tohoku University, Sendai 6-3 Aramaki Aza-Aoba, Aoba-ku, Sendai, Miyagi 980-8579, Japan

³Department of Materials and Synchrotron Radiation Engineering, Graduate School of Engineering, University of Hyogo, Himeji 671-2280, Japan

⁴Division of Materials and Manufacturing Science, Graduate School of Engineering, Osaka University, 2-1 Yamadaoka, Suita, Osaka 565-0871, Japan

^am.todai@niihama-nct.ac.jp, ^bngi98824@icloud.com, ^cqcsx2den9pcibg50nwn1@docomo.ne.jp,

^ddaisuke.tanaka.b7@tohoku.ac.jp, ^et-nagase@eng.u-hyogo.ac.jp,

^fmatsugaki@mat.eng.osaka-u.ac.jp, ^gnakano@mat.eng.osaka-u.ac.jp

Keywords: High entropy alloys (HEAs), Bio metallic materials, microstructure, Young's modulus

Abstract. In recent years, high-entropy alloys (HEAs) have attracted significant attention owing to their remarkable physical properties such as high strength. It has also been reported that HEAs have a high potential as biomaterials. Bcc-type bio-HEAs possess high strength and biocompatibility equivalent to those of pure titanium. Bio-metallic materials require a low Young's modulus, similar to that of natural bone, but the Young's modulus of bio-high entropy alloys has not yet been clarified. Therefore, this study elucidates the relationship between microstructure control and Young's modulus in titanium-based bio-HEAs. The TiNbTaZrMo-based bio-HEAs were composed of two bcc phases. These two microstructures correspond to dendrite and interdendrite structures, respectively. In this study, it was found that by varying the volume fractions of these two microstructures, it is possible to control the strength and Young's modulus.

Introduction

High entropy alloys (HEAs) are defined by their mixing entropy, ΔS_{mix} , and have recently attracted significant attention as a group of materials distinct from conventional metallic materials [1-4]. They exhibit particularly high strengths and are expected to be used as new refractory materials [5]. Our research group has reported that a titanium-based TiZrNbTaMo HEA ($\text{Ti}_{20}\text{Zr}_{20}\text{Nb}_{20}\text{Ta}_{20}\text{Mo}_{20}$) possesses both high strength and biocompatibility comparable to that of pure titanium [6]. This suggests that titanium-based bcc-type high entropy alloys have a high potential as biomaterials. We propose the use of such HEAs for biomedical applications as bio-HEAs [6-12]. In addition to their strength and biocompatibility, metallic biomaterials require a low Young's modulus similar to that of natural bone[13]. In general, metallic materials with a high yield strength tend to have a high Young's modulus, and it is considered that high-strength materials, such as TiZrNbTaMo bio-HEAs, also have a high Young's modulus. The Young's modulus of natural bone is approximately 10 GPa, and when there is a large difference in the Young's modulus between the implanted metallic biomaterials and bone, significant problems (stress shielding) can arise. To use TiZrNbTaMo HEA as a metallic biomaterials (bio-HEAs), it is essential to elucidate and reduce its Young's modulus. Metallic biomaterials must have a balance between a low elastic modulus and sufficient mechanical strength. However, the Young's modulus of bio-HEAs has not yet been determined. Therefore, in this study, the Young's moduli of TiZrNbTaMo -based HEAs were investigated. It was reported that the as-cast TiZrNbTaMo bio-HEA consisted of dendritic and interdendritic microstructures. Both of these structures exhibit a bcc phase, and it has been also reported that the reason for the formation of these

two phases is the the distribution coefficient ($k = C_s / C_L$) of the constituent elements [7,8]. Specifically, during solidification, Ti and Zr are concentrated in the liquid phase, whereas the other elements are concentrated in the solid phase that forms the dendrite phase, resulting in dendritic and interdendritic microstructures with different compositions. It is possible that dendritic and interdendritic microstructures have different elastic properties [14]. Therefore, we focused on the volume fractions of these microstructures and discussed whether it is possible to reduce their Young's modulus. As there have been no previous reports on the control of Young's modulus by systematically varying the volume fractions of the dendritic and interdendritic microstructures, highly valuable insights can be obtained. Furthermore, the alloys desinged were selected using five parameters (ΔS_{mix} , ΔH_{mix} , Ω , δ , and VEC), and $(\text{TiZr})_{2-x}(\text{NbTAZr})_x$ ($x = 0.6$, 1.0 , and 1.4) alloys within the range of high-entropy alloys ($\Delta S_{\text{mix}} \geq 1.5R$) were selected. Here, ΔS_{mix} and ΔH_{mix} represent the entropy of mixing and the enthalpy of mixing, respectively. Ω is dimensionlss parameter and elculated by $T_m \cdot \Delta S_{\text{mix}} / |\Delta H_{\text{mix}}|$. T_m is melting point. δ evalutats the deffrence in the atomic radii of the constituent elements. The details of each parameter are described in Reference 8.

Experimental Procedures

Arc-melted ingots of $(\text{TiZr})_{2-x}(\text{NbTaMo})_x$ ($x = 0.6$, 1.0 , and 1.4) bio-HEAs were prepared by mixing lumps of pure elements. The purity of the Ti, Nb, Ta, Zr, and Mo resources was greater than 3 N (99.9%). To achieve a homogeneous distribution of the constituent elements in the alloys, the alloys were melted more than 10 times and maintained in a liquid state for approximately 120 s during each melting event. The cooling rates during arc melting were roughly estimated to be of the order of $2 \times 10^3 \text{ Ks}^{-1}$ [15]. The uniformity of the alloy microstructure and the absence of unmelted particles were confirmed by OM and SEM observations of the obtained ingots cross-section. The microstructure and constituent phases of the ingots were investigated using X-ray diffraction (XRD) analysis, scanning electron microscopy (SEM), and electron probe microanalysis (EPMA). The Vickers hardness was measured using an Akashi MVK-G1 tester, applying a load of 4.9 kN for 10 seconds. Rectangular specimens were fabricated using an electrical discharge machine, and Young's modulus was measured using the Free Resonance Method by LE-RT from Nihon Techo-Plus Co. Ltd. The specimen size was $40 \text{ mm} \times 5 \text{ mm} \times 1 \text{ mm}$, and the values shown are the averages of three measurements. The error bars of obtained values were $\pm 5 \text{ GPa}$.

Results and Discussion

The XRD measurements of bio-HEAs with $x = 1.0$ shows two bcc phases. These phases correspond to the dendritic and interdendritic phases [8]. In the $x = 0.6$ alloys with increased concentrations of Ti and Zr components, which become enriched in the interdendritic phase, the peak of the interdendritic phase increased, while the peak of the dendritic phase decreased.

Figures 1 and 2 show the optical microscope images and SEM-BSE images of the $(\text{TiZr})_{2-x}(\text{NbTaMo})_x$ ($x = 0.6$, 1.0 , and 1.4) bio-HEAs. All alloys examined in this study were composed of dendritic and interdendritic microstructures, as shown in these figures. Notably, in the $x = 0.6$ alloy, where the concentrations of Ti and Zr, which segregate in the interdendritic phase, increased, the dendritic structure became thinner while the interdendritic microstructure expanded. On the other hand, at $x = 1.4$ alloy, the dendritic microstructure became coarser, and the interdendritic microstructure decreased.

Figures 3 and 4 show the EPMA mappings of $x = 0.6$ and 1.4 alloys. As expected, in both alloys, Ti and Zr are concentrated in the interdendritic regions, while Nb, Ta, and Mo are concentrated in the dendritic regions. Therefore, by varying the composition based on whether the distribution

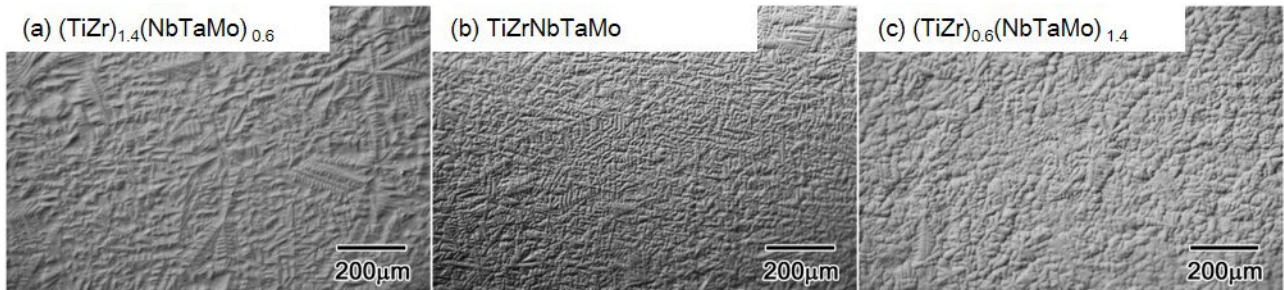


Fig. 1 Optical micrographs of $(\text{TiZr})_{2-x}(\text{NbTaMo})_x$ ($x = 0.6, 1.0$ and 1.4) bio-HEAs.

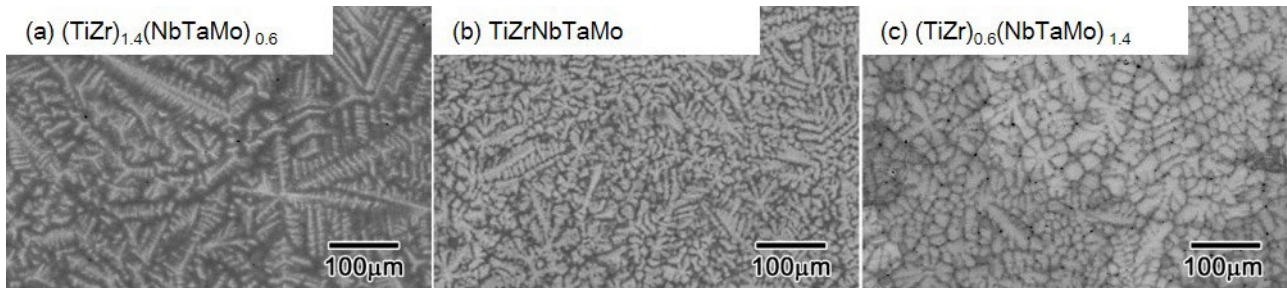


Fig. 2 SEM-BSE images of $(\text{TiZr})_{2-x}(\text{NbTaMo})_x$ ($x = 0.6, 1.0$ and 1.4) bio-HEAs.

coefficient ($k = Cs/CL$) was less than or greater than 1.0, we successfully controlled the volume fraction of the dendritic and interdendritic microstructures.

The results of HV and Young's modulus measurements are shown in Figure 5. The HV value depends on the volume fraction of the dendritic structure and showed the lowest value in the $x = 0.6$ alloy, which has the fewest dendrites. These results are in good agreement with those for the yield stress, indicating that by reducing the dendrites and increasing the volume fraction of the interdendritic microstructure, the yield stress decreases, but the fracture strain improves significantly [7]. Thus, controlling the microstructure by focusing on the volume fraction of the dendritic microstructure is crucial for achieving an optimal balance between strength and ductility.

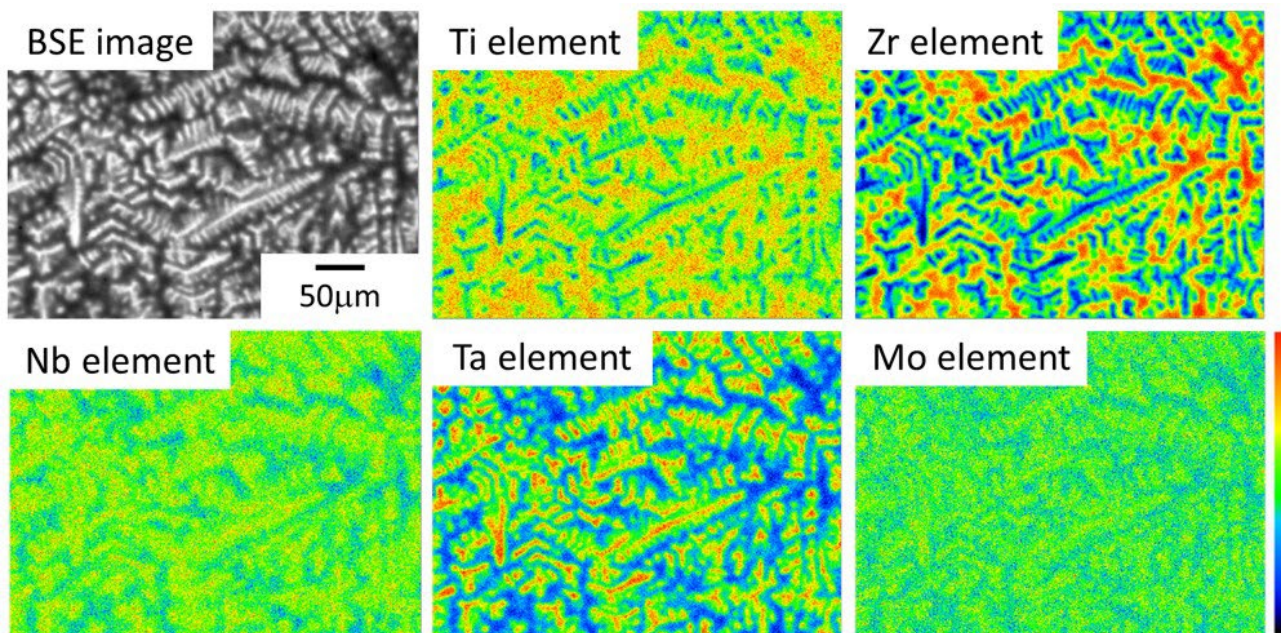


Fig. 3 EPMA mapping of as-cast non-equiautomic $(\text{TiZr})_{2-x}(\text{NbTaMo})_x$ ($x = 0.6$) alloy.

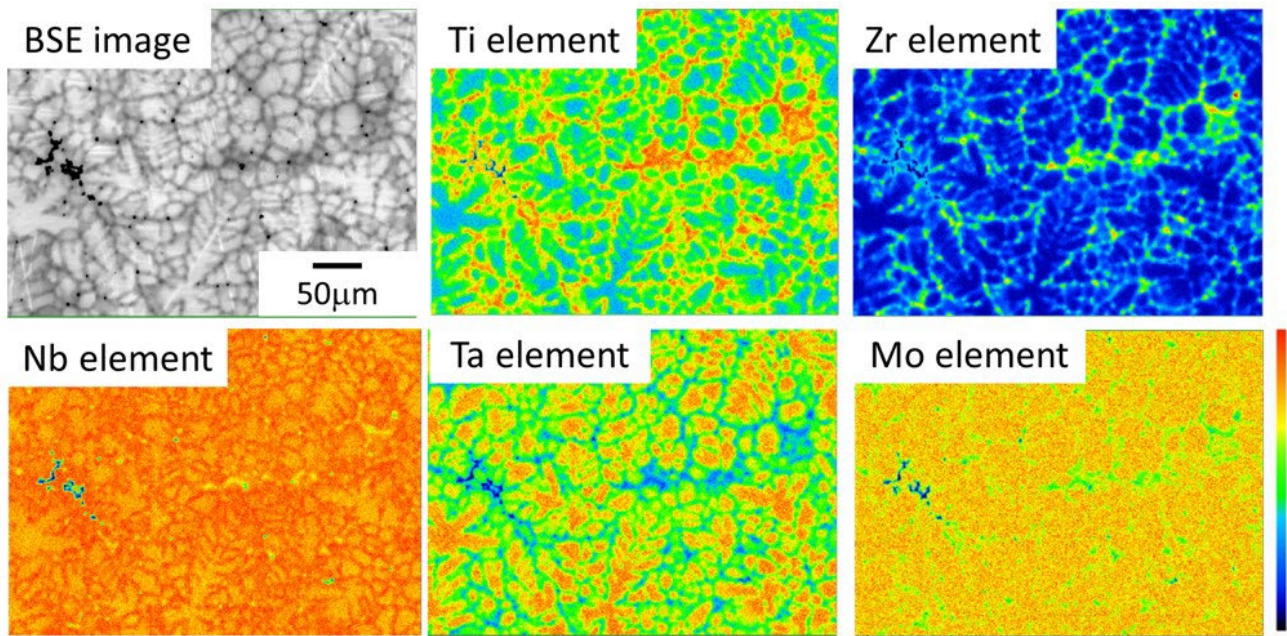


Fig. 4 EPMA mapping of as-cast non-equiautomic $(\text{TiZr})_{2-x}(\text{NbTaMo})_x$ ($x = 1.4$) alloy.

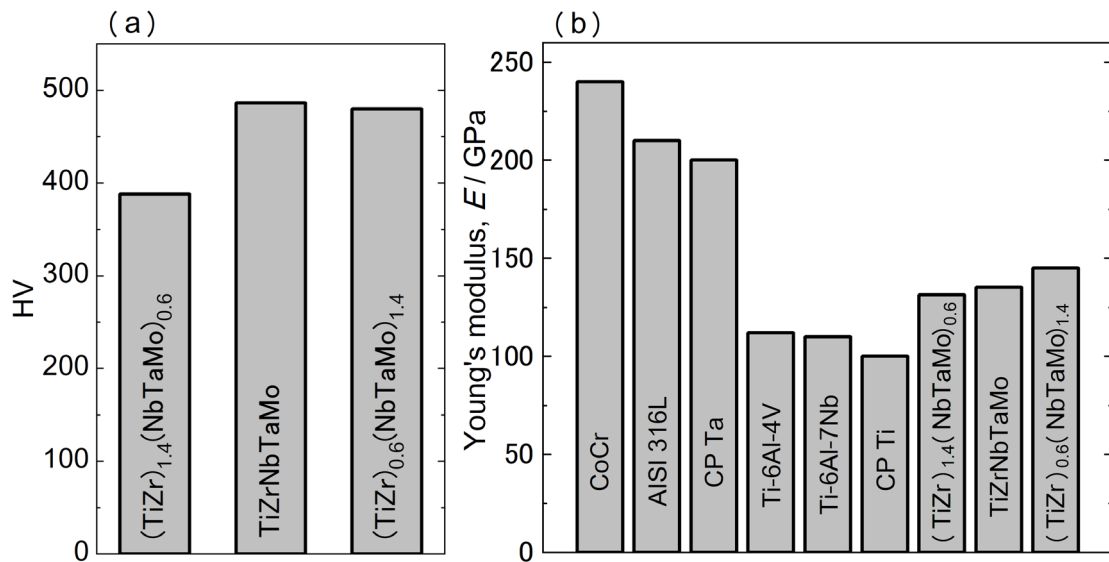


Fig. 5 (a) HV of as-cast non-equiautomic $(\text{TiZr})_{2-x}(\text{NbTaMo})_x$ ($x = 0.6$ 1.0 and 1.4) bio-HEAs. (b) Young's modulus of as-cast non-equiautomic $(\text{TiZr})_{2-x}(\text{NbTaMo})_x$ ($x = 0.6$ 1.0 and 1.4) bio-HEAs compared with the Young's moduli of various practical biomedical metal materials.

The Young's modulus of $(\text{TiZr})_{2-x}(\text{NbTaMo})_x$ bio-HEAs is also influenced by the volume fractions of the dendritic and interdendritic microstructures. All examined compositions exhibited lower Young's modulus values than those of CoCr alloys and AISI316L. In particular, a higher fraction of the interdendritic microstructure correlated with a lower modulus. The alloy with $x = 0.6$ exhibited the lowest Young's modulus and density, attributed to its high Ti and Zr content. Despite their reduced Young's modulus, these $(\text{TiZr})_{2-x}(\text{NbTaMo})_x$ HEAs demonstrate yield strengths exceeding 1000 MPa, highlighting their promise as metallic biomaterials with favorable mechanical properties. For example, further reduction of Young's modulus may be possible by techniques such as single crystallization or texture growth via Additive Manufacturing.

Summary

In this study, we investigated the Young's modulus of non-equiautomic $(\text{TiZr})_{2-x}(\text{NbTaMo})_x$ ($x = 0.6, 1.0$, and 1.4) alloys, focusing on the volume fraction of their dendritic microstructures. We have reached a summary of the present study as follows:

- (1) The $(\text{TiZr})_{2-x}(\text{NbTaMo})_x$ ($x = 0.6, 1.0$ and 1.4) bio-HEAs have two bcc phases with different lattice constants in the as-cast state, which correspond to the dendrite and interdendrite microstructures, respectively.
- (2) The Young's modulus of $(\text{TiZr})_{2-x}(\text{NbTaMo})_x$ ($x = 0.6, 1.0$ and 1.4) bio-HEAs decreased as the volume fraction of the interdendritic microstructure increased.

Acknowledgements

This work was partially supported by JSPS KAKENHI (grant numbers 23K04426); the research grant of Daiichi Kigenso Kagaku Kogyo; the light metal educational foundation and the Takahashi Industrial and Economic Research Foundation.

References

- [1] B. Cantor, I.T.H. Chang, P. Knight, A.J.B. Vincent, Microstructural development in equiautomic multicomponent alloys, *Mater. Sci. Eng., A* 375-377 (2004) 213–218.
- [2] J.W. Yeh, S.K. Chen, S.J. Lin, J.Y. Gan, T.S. Chin, T.T. Shun, C.H. Tsau, S.Y. Chang, Nanostructured high-entropy alloys with multiple principal elements: novel alloy design concepts and outcomes, *Adv. Eng. Mater.* 6 (2004) 299–303.
- [3] B.S. Murty, J.-W. Yeh, S. Ranganathan, *High-entropy Alloys*, first ed., Elsevier, 2014.
- [4] O.N. Senkov, J.M. Scotta, S.V. Senkova, D.B. Miracle, C.F. Woodward, Microstructure and room temperature properties of a high-entropy TaNbHfZrTi alloy, *J. Alloy. Compd.* 509 (2011) 6043–6048.
- [5] O.N. Senkov, G.B. Wilks, J.M. Scott, D.B. Miracle, Mechanical properties of $\text{Nb}_{25}\text{Mo}_{25}\text{Ta}_{25}\text{W}_{25}$ and $\text{V}_{20}\text{Nb}_{20}\text{Mo}_{20}\text{Ta}_{20}\text{W}_{20}$ refractory high entropy alloys *Intermetallics* 19 (2011) 698–706.
- [6] M. Todai, T. Nagase, T. Hori, A. Matsugaki, A. Sekita, T. Nakano, Novel TiNbTaZrMo high-entropy alloys for metallic biomaterials, *Scripta Materialia* 129 (2017) 65–68.
- [7] T. Hori, T. Nagase, M. Todai, A. Matsugaki, T. Nakano, Development of Non-equiautomic Ti-Nb-Ta-Zr-Mo High-Entropy Alloys for Metallic Biomaterials, *Scripta Materialia* 172 (2019) 83–87.
- [8] T. Nagase, M. Todai, T. Hori, T. Nakano, Microstructure of equiautomic and non-equiautomic Ti-Nb-Ta-Zr-Mo high-entropy alloys for metallic biomaterials, *Journal of Alloys and Compounds*, 753 (2018) 412–421.
- [9] T. Nagase, M. Todai, S. Ichikawa, A. Matsugaki, T. Nakano, Alloy Design and Solidification Microstructure of Ti-Zr-Hf-Ag-V Multi-Component Alloys with a Dual Bcc Structure, *Materials Transactions*, 65[9] 2024 1041–1048.
- [10] T. Nagase, M. Todai, T. Nakano, Liquid phase separation in Co-Cr-Fe-Mn-Ni-Ag and Co-Cr-Fe-Mn-Ni-Cu High entropy alloys, *Crystals* 10 (2020) 527
- [11] T. Nagase, M. Todai, T. Nakano, Development of Co-Cr-Mo-Fe-Mn-W and $\text{Co-Cr-Mo-Fe-Mn-W-Ag}$ High-Entropy Alloys Based on Co-Cr-Mo alloys, *Materials Transactions* 61 (2020) 567–576.

- [12] T. Nagase, M. Todai, T. Nakano, Development of Ti-Zr-Hf-Y-La high-entropy alloys with dual hexagonal-close-packed structure, *Scripta Materialia* 186 (2020) 242–246.
- [13] M. Todai, K. Hagihara, T. Ishimoto, K. Yamamoto, T. Nakano, Development of Single Crystalline Bone Plate with Low Young's Modulus Using Beta-type Ti-15Mo-5Zr-3Al Alloy, *Tetsu-to-Hagane* 101 (2015) 501–505.
- [14] N.E. Koval, J.I. Juaristi, R.D. Muino, M. Alducin, Elastic properties of the TiZrNbTaMo multi-principal element alloy studied from first principles, *Intermetallics* 106 (2019) 130–140.
- [15] T. Nagase, M. Matsumoto, Y. Fujii, Microstructure of Ti-Ag immiscible alloys with liquid phase separation, *J. of Alloys and Compounds* 738 (2018) 440–447.